communications biology

Article

https://doi.org/10.1038/s42003-024-06747-9

Polarly localized Bro1 domain proteins regulate PIN-FORMED abundance and root gravitropic growth in *Arabidopsis*

Check for updates

Yakun Peng[1], Kangkang Ji[1], Yanbo Mao[1], Yiqun Wang[2], Barbara Korbei[3], Christian Luschnig[3], Jinbo Shen[4], Eva Benková[2], Jiří Friml[2] & Shutang Tan[1]

The developmental plasticity of the root system plays an essential role in the adaptation of plants to the environment. Among many other signals, auxin and its directional, intercellular transport are critical in regulating root growth and development. In particular, the PIN-FORMED2 (PIN2) auxin exporter acts as a key regulator of root gravitropic growth. Multiple regulators have been reported to be involved in PIN2-mediated root growth; however, our information remains incomplete. Here, we identified ROWY Bro1-domain proteins as important regulators of PIN2 sorting control. Genetic analysis revealed that *Arabidopsis rowy1* single mutants and higher-order *rowy1 rowy2 rowy3* triple mutants presented a wavy root growth phenotype. Cell biological experiments revealed that ROWY1 and PIN2 colocalized to the apical side of the plasma membrane in the root epidermis and that ROWYs are required for correct PM targeting of PIN2. In addition, ROWYs also affected PIN3 protein abundance in the stele, suggesting the potential involvement of additional PIN transporters as well as other proteins. A global transcriptome analysis revealed that *ROWY* genes are involved in the Fe^{2+} availability perception pathway. This work establishes ROWYs as important novel regulators of root gravitropic growth by connecting micronutrient availability to the proper subcellular targeting of PIN auxin transporters.

Land plants utilize the root system to support themselves and to absorb water and nutrients from the soil. Root growth and development require the coordination of internal signals and environmental cues and exhibit highly adaptive plasticity under different environmental conditions. The phytohormone auxin (with the major natural form being indole-3-acetic acid (IAA)) and the related molecular framework play fundamental roles in almost every aspect of plant life, including root growth and developmental regulation[1]. Genetic studies have established the molecular network for auxin biosynthesis[2–4], transport[5,6], and signaling[7,8], which cooperate in a multitude of auxin functions.

For IAA biosynthesis, the TRYPTOPHAN AMINOTRANSFERASE OF ARABIDOPSIS (TAA1)/TRYPTOPHAN AMINOTRANSFERASE RELATED PROTEIN (TAR) and YUCCA (YUC) enzymes catalyze the conversion of tryptophan to indole-3-pyruvic acid (IPyA) and subsequently IAA, which is a major pathway in plants[2,9–11]. In addition, multiple modifications of IAA, such as oxidation or conjugation to amino acids, control IAA homeostasis in plants[2]. The nuclear TRANSPORT INHIBITOR RESPONSE1 (TIR1)/AUXIN SIGNALLING F-BOX (AFB)-AUXIN/INDOLE-3-ACETIC ACID (Aux/IAA) pathway mediates auxin function in transcriptional regulation[7,12] and in nontranscriptional rapid responses related to the regulation of root growth[13–15]. Recently, studies have revealed that cell-surface AUXIN BINDING PROTEIN1 (ABP1)-TRANSMEMBRANE KINASE (TMK)-based auxin perception results in rapid cellular auxin responses through global modulation of the phosphoproteome[16].

Directional intercellular auxin transport, namely, polar auxin transport (PAT), is a key feature of auxin action. The plasma membrane (PM)-localized PIN-FORMED (PIN) family of auxin transporters pump auxin out of the cell, playing essential roles in PAT[17–21]. Intriguingly, PIN transporters reside asymmetrically at the PM, and this polarity of PIN proteins determines the directionality of intercellular auxin flow, which is crucial in many patterning processes as well as in asymmetric growth during tropic responses[5,6,22]. ABC transporters have also been reported to be involved in

[1]MOE Key Laboratory for Cellular Dynamics, Center for Advanced Interdisciplinary Science and Biomedicine of IHM, Hefei National Laboratory for Physical Sciences at the Microscale, Division of Life Sciences and Medicine, University of Science and Technology of China, Hefei, China. [2]Institute of Science and Technology Austria (ISTA), Am Campus 1, Klosterneuburg, Austria. [3]Department of Applied Genetics and Cell Biology, Institute of Molecular Plant Biology, University of Natural Resources and Life Sciences, Vienna (BOKU), Muthgasse 18, Wien, Austria. [4]State Key Laboratory of Subtropical Silviculture, Zhejiang A&F University, Hangzhou, China. e-mail: sttan@ustc.edu.cn

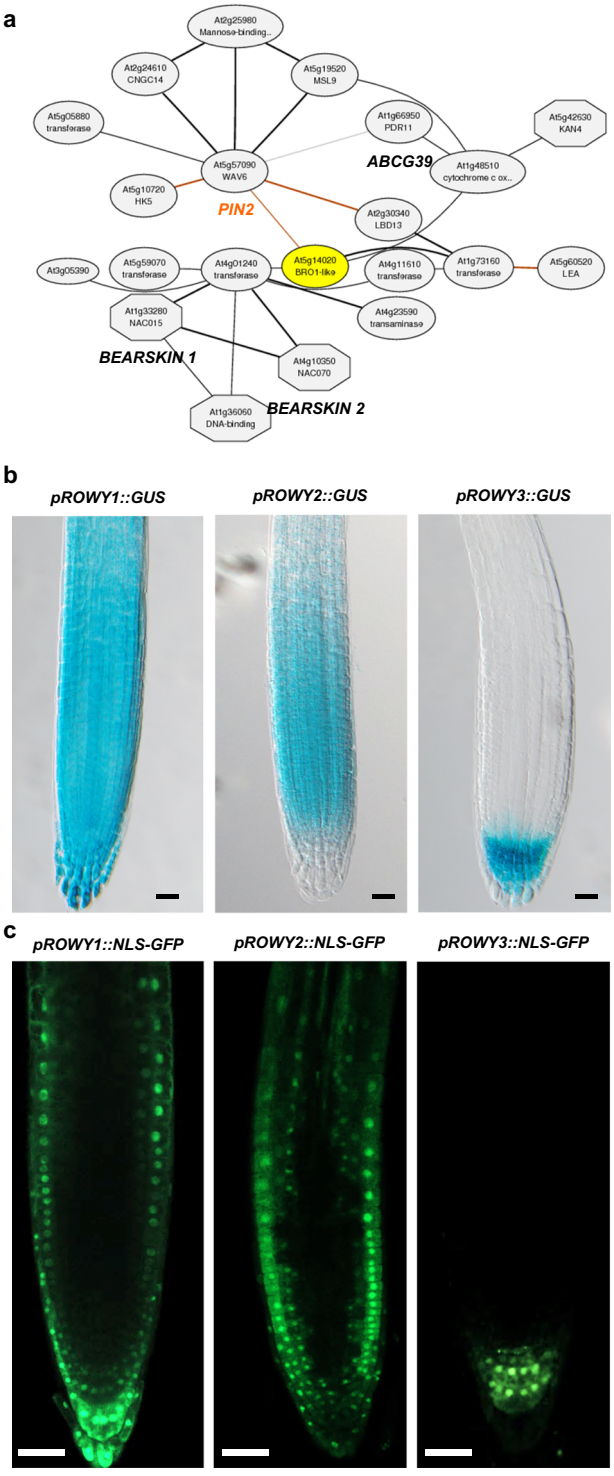

Fig. 1 | *ROWY1* is a candidate regulatory gene for root growth and development. **a** Coexpression analysis of the *PIN2* gene via the ATTED-II (http://atted.jp) database identified candidate genes that may be involved in PIN2 regulation of root growth and development. **b** Expression patterns of *ROWYs* revealed by *pROWY1::GUS, pROWY2::GUS*, and *pROWY3::GUS* reporter transgenic lines in *Arabidopsis* roots. Five-day-old *pROWYx::GUS* seedlings grown on plates were selected for GUS staining and imaged via light microscopy. $n = 25$, 17, 20. Scale bars, 50 μm. The experiments were repeated four times independently, with similar results obtained. **c** Expression patterns of *ROWYs* revealed by *pROWY1::NLS-GFP, pROWY2::NLS-GFP*, and *pROWY3::NLS-GFP* reporter transgenic lines in *Arabidopsis* roots. Five-day-old *pROWYx::NLS-GFP* seedlings grown on plates were imaged via confocal laser scanning microscopy (CLSM). Laser wavelength, 488 nm, 5.00%; 0.0% offset; detector gain, 580 V. $n = 21$, 22, and 19, respectively. Scale bars, 50 μm. The experiments were repeated three times independently, with similar results obtained.

auxin export[23,24], but recent work has suggested that ABCB19 is a major brassinosteroid transporter[25]. Moreover, AUXIN1 (AUX1)/LIKE AUXINs (LAXs) are auxin importers[26]. In addition, intracellular auxin transporters, such as PIN-LIKES (PILS), tonoplast-associated WALLS ARE THIN1 (WAT1), and TOB1 (TRANSPORTER OF IBA1), potentially control free auxin homeostasis via subcellular compartmentalization inside the cell[5,6].

There are eight members of the PIN family of transporters: PIN1 ~ PIN4 and PIN7 localize to the PM, and PIN5, PIN6, and PIN8 reside in the ER (with PIN6 also at the PM), with the latter participating in intracellular auxin transport[5,27]. Among those PIN transporters, PIN2 (also known as AGRAVITROPIC1/AGR1, ETHYLENE INSENSITIVE ROOT1/EIR1 and WAV6) controls root growth and development[28], and it is expressed mainly in the epidermis, cortex, and lateral root cap in the root meristem. Loss-of-function *pin2* mutants exhibit agravitropic roots, and a critical function for correct plasma membrane targeting and the intracellular distribution of PIN2 for directional root growth is underlined by characterization of *trans*-acting regulators. AGC [named cAMP-dependent (PKA) and cGMP-dependent protein kinase (PKG) and protein kinase C (PKC)] kinases, such as PINOID (PID) and WAVY ROOT GROWTHs (WAGs), regulate the polarity and activity of the PIN2 protein by phosphorylating its cytosolic loop[29–31]. The BTB family E3 ligases MACCHI-BOU4 (MAB4)/ENHANCER OF PID (ENP)/NAKED PINS IN YUCCA-LIKE1 (NPY1) protein and homologous MELs (MAB4/ENP/NPY1-LIKEs) are essential for the establishment and maintenance of apical PIN2 polarity in the root epidermis[31,32]. Similarly, recent studies imply that WAVY GROWTH3 (WAV3) and WAV3-LIKE E3 ligases are critical regulators of PIN2 apical polarity and thus root gravitropism[22,33].

Multiple hormonal and nutrient signaling pathways converge on PIN2 to regulate growth[6,34], including the cytokinin[35], ethylene[22,28], brassinosteroid[36,37], salicylic acid[38–42], abscisic acid[43,44], jasmonic acid[45], strigolactone[46], and mTOR and nitrogen signaling pathways[47]. In addition, auxin itself also regulates PIN PM localization, forming a feedback loop controlling PIN abundance at the PM[16,48–50].

In this study, we revealed that *Arabidopsis* Bro1 domain proteins, ROOT WAVY GROWTHs (ROWYs), modulate root growth and development by positively regulating PIN2 stability and subcellular dynamics. Specifically, our work provides novel insights into PIN-mediated polar auxin transport and related root patterning processes and links PIN2 function to variations in micronutrient availability.

Results

Coexpression analysis identified *ROWY1* as a putative regulatory gene that acts in conjunction with *PIN2* in *Arabidopsis* roots

PIN2 is a key regulator of root growth and development[22,28,31]. To identify putative regulatory genes involved in *PIN2*-mediated root growth and development, we performed a coexpression analysis in the ATTED-II (http://atted.jp) database (Fig. 1a). Multiple coexpressed genes, such as *CNGC14* and *BEARSKIN1/2* (Fig. 1a), were previously reported to be involved in root development or gravitropism[51]. *AT5G14020* (hereafter named *ROOT WAVY GROWTH1*, *ROWY1*, previously also named *BRo1-domain protein As FREE1 suppressor, BRAF*) encodes a Bro1-domain protein, which was previously identified as a regulator of the ESCRT-I-mediated sorting of plasma membrane cargo via competitively binding to the VPS23 subunit[52]. However, the biological functions of *ROWY1* have not been reported previously.

In the *Arabidopsis* genome, there are three genes encoding ROWY1 and its closest homologs: *AT5G14020* (*ROWY1*), *AT1G17940* (*ROWY2*), and *AT1G73390* (*ROWY3*, previously also named *AtBro1*)[53] (Supplementary Figs. 1 and 2). Phylogenetic analysis revealed that ROWYs are homologs of ALIX (Supplementary Figs. 1 and 3), which is a critical regulator of the ESCRT pathway in eukaryotes. The available single-cell RNA-seq data

indicated that *ROWY1, ROWY2*, and *ROWY3* were expressed in root cells (Supplementary Fig. 4). To further study the expression patterns of the *ROWY* genes, we constructed promoter-driven GUS reporter lines. GUS staining of the resulting lines revealed that *ROWY1* ~ *ROWY3* were expressed in multiple tissues (Supplementary Fig. 5), and specifically, they were detected in root meristems (Fig. 1b, c). Notably, although all three *ROWY* genes are expressed in the root, GUS staining revealed some differences in the expressed cell layers compared with the single-cell RNA-seq data, which also reflects the requirement for cell biological verification for high-throughput data. In contrast to the constitutive pattern observed from the single-cell RNA-seq data, *ROWY3* was predominantly expressed in root columella cells and lateral root cap cells, whereas *ROWY2* was expressed in the division and elongation zones. Together with the results from the transcriptomics analysis, these findings indicate that *ROWY* functions in root meristems.

The *rowy1 rowy2 rowy3* triple mutant results in a wavy growth root phenotype in *Arabidopsis*

To study the biological functions of the *ROWY* genes, T-DNA insertional mutants, *rowy1-1, rowy1-2, rowy2-1, rowy2-2, rowy3-1*, and *rowy3-2*, were obtained and verified via PCR analysis (Supplementary Fig. 6a, b). Further RT-qPCR and RT-PCR analyses revealed that *rowy1-1, rowy1-2, rowy2-1*, and *rowy2-2* were knockout mutants, whereas *rowy3-1* and *rowy3-2* appeared to represent knockdown alleles (Supplementary Fig. 7a, b).

Phenotypic analysis revealed that *rowy1-1* and *rowy1-2* single mutants presented increased root waviness when grown on vertically oriented nutrient plates, whereas *rowy2-1, rowy2-2, rowy3-1*, and *rowy3-2* did not (Supplementary Fig. 8a–c). Double and triple mutants were generated by crossing, and a more pronounced root wavy growth phenotype was observed for the *rowy1-1 rowy2-2 rowy3-2* (hereafter referred to as *rowy123*, used for further analyses) and *rowy1-2 rowy2-1 rowy3-1* triple mutants, suggesting functional redundancy of the *ROWY* genes (Fig. 2a–f, Supplementary Fig. 8d–f, and Supplementary Fig. 9). Specifically, the primary root of *rowy123* was longer than that of wild-type Col-0 (Fig. 2c), and the root tip angles of *rowy123* were more variable than those of wild-type Col-0 (Fig. 2e, f). Consistent with the wavy root phenotype, *rowy123* mutants presented a smaller root gravitropic index value (distance/primary root length) than did Col-0 (Fig. 2c, d, and Supplementary Fig. 9). To study the role of *ROWY* genes in the root gravitropic response in more detail, vertically grown seedlings were turned 90°, followed by determination of the kinetics of root tip reorientation over time. This analysis revealed that the roots of *rowy123* bent more rapidly than those of Col-0 did (Supplementary Fig. 10). Notably, the wavy root growth phenotype of *rowy123* plants was also observed in the dark (Supplementary Fig. 11). Therefore, we speculated that the wavy root growth phenotype of *rowy123* might be due to both defects in gravitropic growth and its faster growth rate. Notably, the gravitropic phenotype of *rowy123* mutants is different from that of *pin2* mutants, which usually bend randomly under gravistimulation conditions. We speculate that the wavy root phenotype of *rowy123* might be due to a defect in bending termination during gravitropism.

To further analyze the expression and function of the *ROWY* genes in wavy root growth, the transgenic lines *rowy123 pROWY1::ROWY1-GFP* and *rowy123 pROWY2::ROWY2-GFP* were generated. Analysis of the root phenotype at the seedling stage revealed that the *pROWY1::ROWY1-GFP* transgene rescued the root phenotype of *rowy123* in terms of the wavy phenotype (Supplementary Fig. 12a–d), whereas *pROWY2::ROWY2-GFP* did not (Supplementary Fig. 12e–h). This finding is consistent with the fact that the *rowy1* mutants presented a root wavy phenotype, whereas the *rowy2* and *rowy2 rowy3* mutants did not, suggesting a predominant role of *ROWY1* in controlling root growth.

The ROWY1 protein is localized to the apical plasma membrane domain in root epidermal cells in *Arabidopsis*

To study the subcellular localization of ROWY1, a complemented *rowy123 pROWY1::ROWY1-YFP* transgenic line was used for analysis. Imaging via confocal laser scanning microscopy (CLSM) revealed that ROWY1-YFP is expressed mainly in the epidermis, lateral root cap, and columella cells in the root meristem (Fig. 3a). Notably, both ROWY1-YFP and ROWY1-GFP exhibited polar subcellular localization enriched at the apical side of the root meristem epidermis cells (Fig. 3a, b). A comparison of the signals from the *pROWY1::ROWY1-GFP* and *pROWY2::ROWY2-GFP* lines with those from the pPIN2::PIN2-GFP (*eir1-4*) line in root meristem epidermis cells as a control revealed striking overlap, with predominant enrichment of reporter signals at the apical domain of the plasma membrane (PM) (Fig. 3b, c and Supplementary Fig. 13).

It was reported previously[52] that ROWY1/BRAF showed dual localization at both the PM and MVB/LE/PVC, and the PM targeting of ROWY1 might be due to S-acylation of cysteine 3 (C3). Consistently, treatment with the S-acylation inhibitor 2-BP (2-bromopalmitate) abolished the PM localization of ROWY1-GFP, suggesting that S-acylation might indeed be essential for ROWY1 PM targeting (Supplementary Fig. 14a). Further analysis of the *pROWY1::rowy1*^{C3A}*-GFP* allele, with the presumptive C3 S-acylation site substituted by alanine (A), demonstrated that mutant rowy1^{C3A}-GFP failed to localize to the PM, confirming the importance of the C3 residue for ROWY1 subcellular localization (Supplementary Fig. 14a). Remarkably, the transgene harboring *rowy1*^{C3A}*-GFP* rescued the wavy root phenotype of *rowy123* but failed to rescue *rowy123* root elongation defects, suggesting that discernible subcellular ROWY1 localization impacts distinct aspects of *rowy123* root growth defects (Supplementary Fig. 14b–d). Given that the wild-type version of the *pROWY1::ROWY1-GFP* transgene partially rescued the root elongation phenotype of *rowy123* (Supplementary Fig. 12a–d), we speculate that PM targeting is required for its full function. In line with observations suggesting that ROWY1 functions as a negative regulator of the ESCRT complex at MVB/LE/PVC[52], we speculate that both the PM and MVB/LE/PVC subcellular localizations of ROWY1 contribute to its role in controlling root growth.

Involvement of *ROWY* genes in the regulation of auxin-mediated root growth in *Arabidopsis*

To examine the functional relationship between ROWY1 and PIN2, a *pROWY1::ROWY1-YFP pPIN2::PIN2-mCherry (eir1-4)* line was generated. Imaging via CLSM revealed that the ROWY1-YFP and PIN2-mCherry signals strongly overlapped at the apical plasma membrane domain of the root epidermis cells, which is consistent with regulatory crosstalk between these proteins (Fig. 4a, b). Notably, ROWY1-YFP was also expressed in and localized to the apical side of the cortex layer in the elongation zone but not in the division zone, where PIN2, however, localized to the basal side. These findings suggest that ROWY1 might have additional functions in root development. To explore the genetic interaction between *ROWYs* and *PIN2*, a cross was made for *rowy123* and *eir1-4* (also named *pin2-T*). The root phenotype of *rowy123 eir1-4* revealed epistasis of *eir1-4* to *rowy123*, suggesting that the *ROWYs* function upstream of *PIN2* (Fig. 4c–e). Consistently, pharmacological treatments with salicylic acid (SA), ibuprofen (IBU), TIBA or NPA, compounds that interfere with polar auxin transport, enhanced the agravitropic root phenotype of *rowy123*, substantiating a function for ROWYs upstream of elements of the auxin transport machinery (Supplementary Fig. 15).

We next introduced the *pPIN2::PIN2-Venus (eir1-4)* reporter into *rowy123* to test the consequences of a loss of *ROWY* genes on PIN2 reporter fate. Notably, the signal intensity of pPIN2::PIN2-Venus *(eir1-4)* was markedly lower in *rowy123* than in the wild-type controls (Fig. 4f–i). The assessment of PIN2-Venus signal distribution in the root meristem epidermis cells revealed more intracellular signals in *rowy123* than in the wild type (Fig. 4h–j), which is indicative of deficiencies in PIN2 intracellular trafficking. Brefeldin A (BFA) treatment predominantly affects the plasma membrane targeting of PINs by interfering with steps in the secretory pathway and with protein recycling between the plasma membrane and the endomembrane system[16,48–50]. As a result, BFA causes the accumulation of cargo proteins in intracellular so-called BFA bodies. While there was less PIN2-GFP in *rowy123* at the PM, the BFA body in *rowy123* was smaller than

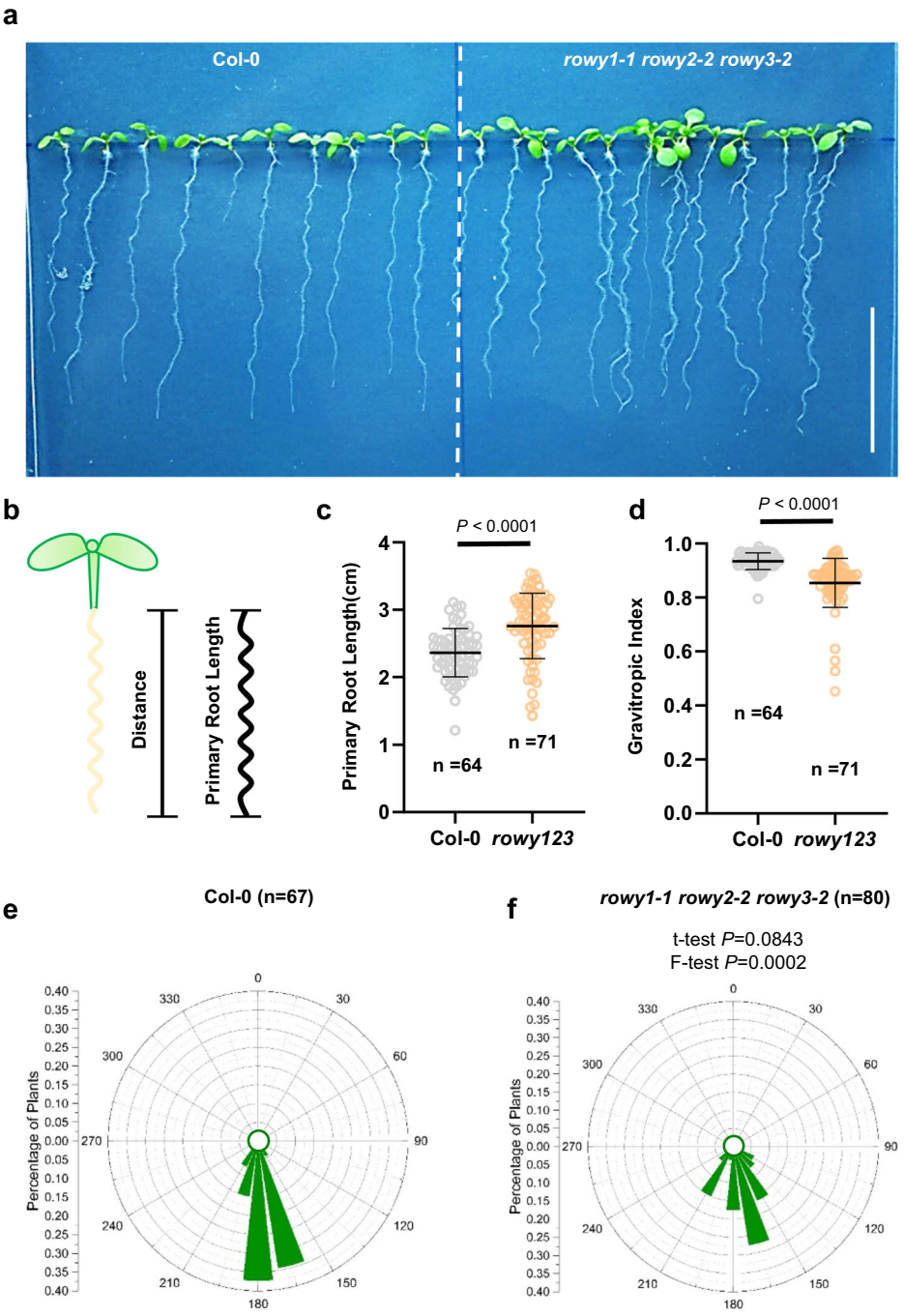

Fig. 2 | The *rowy123* triple mutant presented a wavy root growth phenotype. a Representative images showing the wavy root phenotypes of 7-day-old Col-0 and *rowy1-1 rowy2-2 rowy3-2* (referred to as *rowy123*) seedlings grown on MS media. Scale bars, 2 cm. **b** The wavy growth phenotype of the primary root (primary root length and distance) was evaluated. The distance:primary root length ratio (i.e., the gravitropic index, GI) was measured to indicate the degree of bending. **c** Deficiency of *ROWYs* led to longer roots than those of wild-type Col-0. **d** Deficiency of ROWYs led to a decline in the GI value. Seven-day-old Col-0 seedlings were used for these measurements. The data are presented as the means ± SDs. *n* values are indicated. *P* values were calculated by comparing Col-0 and *rowy123* with a two-tailed *t* test. **e**, **f** Mutations of *ROWYs* interfered with root gravitropism. The angles of the primary root tips of 7-day-old Col-0 and *rowy123* seedlings were measured and are shown as polar histograms. *n* values are indicated. The experiments were repeated three times independently, with similar results obtained.

that in the WT (Supplementary Fig. 16a, b), suggesting a defect in the intracellular trafficking of the PIN2 cargo protein. Further treatment with the PI3K inhibitor wortmannin (Wm) also revealed a similar intracellular distribution of the PIN2 cargo protein (Supplementary Fig. 16c, d). In addition, the deficiency of ROWYs led to a decrease in the abundance of PIN2 at the PM in both epidermal cells and cortical cells in the elongation zone, and a similar decrease was also observed in lateral root cap (LRC) cells (Supplementary Fig. 17a–f).

Further analysis of *pPIN3::PIN3-GFP* revealed that there was a decrease in the PIN3-GFP signal in the stele in *rowy1-1 rowy3-2*, whereas the PIN3-GFP fluorescence in the columella cells of the root cap in *rowy1-1 rowy3-2* was similar to that of the WT (Supplementary Fig. 18a, b). In addition, there was no obvious change in *pPIN7::PIN7-GFP* in *rowy123* (Supplementary Fig. 18c, d). Therefore, we speculate that *ROWY* genes might be involved in the endomembrane trafficking of a subset of PIN cargo proteins, among which PIN2 shows major changes. The decrease in PIN3 protein and possibly additional PIN members in the stele might contribute to rootward auxin transport and thus auxin accumulation in the root tip. Moreover, whether columellar cell-expressed PIN members might also play roles in the auxin stream from the root cap to the elongation zone requires further investigation.

Given the essential roles of PIN2 in mediating both auxin flux from the root tip to the root elongation zone and auxin reflux to the root tip, we asked whether exogenously applied auxin could rescue root growth deficiencies that arise as a consequence of impaired PIN2 distribution in *rowy123*. Indeed, auxin treatments rescued the wavy growth phenotype of *rowy123* (Fig. 5a–c), suggesting that altered auxin homeostasis resulting from loss of the *ROWY* genes could contribute to *rowy123* phenotypes. To further test this hypothesis, we introduced a *DR5rev::GFP* auxin-responsive reporter into *rowy123* by crossing. Quantitative CLSM analysis revealed a decrease in

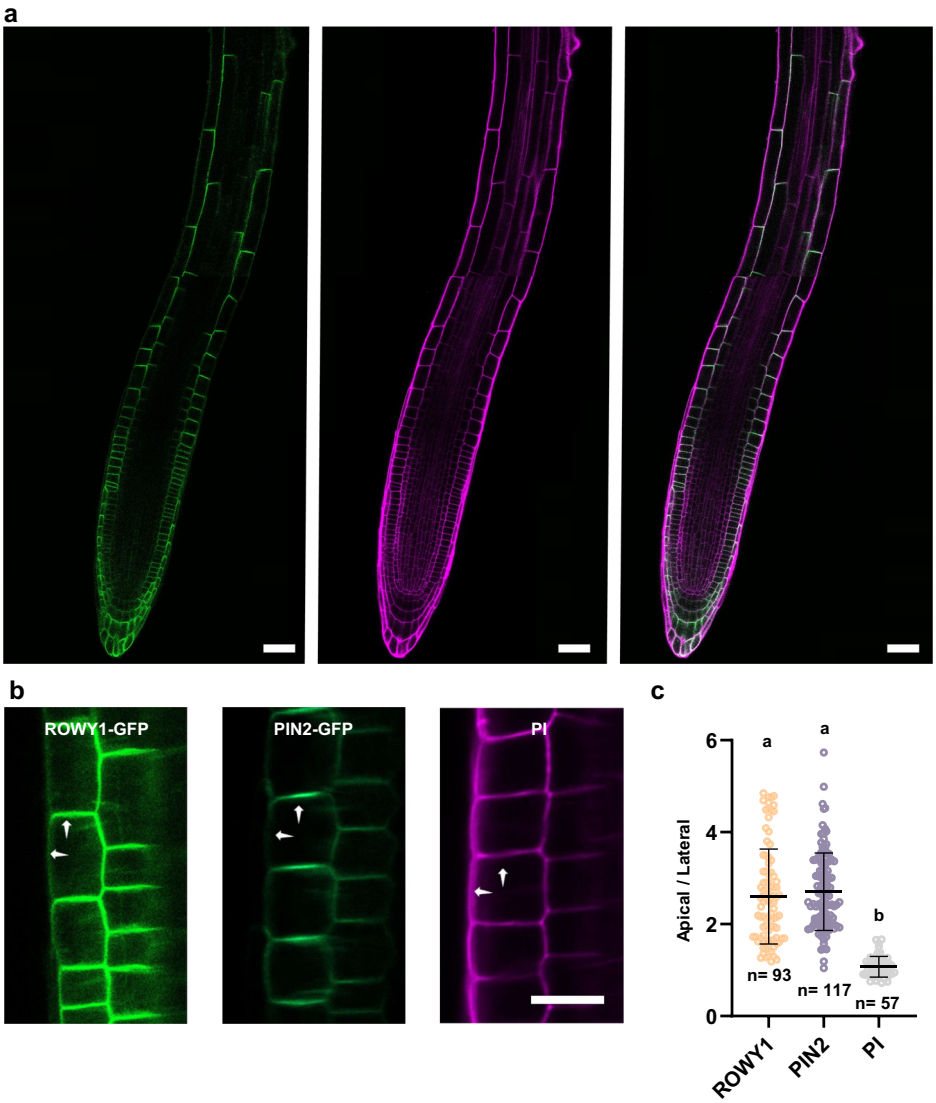

Fig. 3 | ROWY1 exhibited polar localization at the apical side of root epidermal cells. a Subcellular localization of ROWY1-YFP (left) and PI staining (middle) in primary roots of 5-day-old *pROWY1::ROWY1-YFP* seedlings via CLSM. Merged image of ROWY1-YFP and PI staining (right). Scale bars, 20 μm. **b** Subcellular localization of ROWY1-GFP. Arrowheads indicate the position of fluorescence intensity quantification. Primary roots of 5-day-old *pROWY1::ROWY1-GFP, pPIN2::PIN2-GFP*, and Col-0 seedlings were imaged via CLSM. PIN2-GFP was used as a positive control, and PI staining was used as a negative control. ROWY1-GFP: laser wavelength, 488 nm, 4.00%; 0.0% offset; detector gain, 700 V. PIN2-GFP: laser wavelength, 488 nm, 4.00%; 0.0% offset; detector gain, 700 V. PI: laser wavelength, 495 nm, 4%; 0.0% offset; detector gain, 700 V. Scale bar, 20 μm. The experiments were repeated three times independently, with similar results obtained. **c** The apical:lateral ratio of the fluorescence signal was measured to indicate polar localization. Data are presented as the means ± SDs; $n = 93$, 117, and 57 cells from 5 to 10 seedlings, respectively. Different letters represent significant differences; $P < 0.05$; one-way ANOVA with multiple comparisons.

DR5 signal intensity in *rowy123*, which was partially rescued by external auxin application (Fig. 5d, e). These results suggest that the wavy root growth phenotype of *rowy123* might be due to lower auxin levels or a lower capability to maintain maximal auxin, potentially arising as a consequence of alterations in PIN2- and additional PINs-mediated directional auxin transport. Further analysis of the *DR5rev::GFP* reporter in the root gravitropic response by 90° reorientation revealed a decrease in DR5 relocation at 4 h, suggesting a defect in shootward auxin transport (Supplementary Fig. 19). This is in line with the decreased PIN2 levels in the PM in the lateral root cap cells.

The Fe^{2+} deficiency-responsive pathway regulates root wavy growth in *Arabidopsis*

Our results suggest that *ROWY* genes play an essential role in regulating root growth and development in *Arabidopsis*. However, the upstream signaling of *ROWY* genes is still unknown. To test this hypothesis, an RNA-seq experiment was performed with Col-0 and *rowy123* seedlings. Approximately 107 differentially expressed genes (DEGs) were identified in *rowy123* compared with those in Col-0, of which 32 genes were upregulated and 75 genes were downregulated (Fig. 6a, b, and Supplementary Data 1). GO analysis suggested that multiple Fe deficiency-related genes were enriched in these DEGs. For example, *VACUOLAR IRON TRANSPORTER-LIKE1 (AtVTL1), AtVTL2*, and *AtVTL5*[54], which encode for proteins that catalyze Fe transport into vacuoles into vacuoles into vacuoles, were upregulated in *rowy123* mutants. To further test whether Fe deficiency is involved in the regulation of root growth and development, *Arabidopsis* Col-0 and *rowy123* seedlings were grown on $+Fe^{2+}$ (normal MS media) and $-Fe^{2+}$ media, respectively. The results revealed that Col-0 seedlings presented a wavy root phenotype on $-Fe^{2+}$ MS media, similar to that of *rowy123* plants on normal MS media (Fig. 6c–e). A growth assay of the gravitropic response revealed that Fe^{2+} deficiency led to faster gravitropic growth, which is similar to the phenotype of *rowy123* (Supplementary Fig. 20a, b). Further analysis of *PIN2::PIN2-Venus* and the *DR5rev::GFP* auxin-responsive reporter revealed that Fe^{2+} deficiency led to a decrease in the PIN2 signal and an increase in the DR5 signal in the root tip (Fig. 6f, g, and Supplementary Fig. 20c, d). Therefore, we hypothesized that *ROWY* genes might be involved in iron-modulated root growth and development.

Discussion

Auxin plays essential roles in regulating plant growth and development. The root system architecture is largely shaped by various environmental cues and intrinsic signals, and auxin is a central signal. The root-waving phenotype is reportedly regulated by exogenous mechanical cues as well as endogenous hormones and proteins, such as the microtubule cytoskeleton[55]. Here, we revealed that the *ROWY1* gene is a key regulator of root waving. Our data suggest that *ROWY1*, possibly together with other *ROWY* members, is involved in PIN2-mediated root gravitropic growth. In line with the enhanced wavy growth phenotype in the *rowy123* triple mutant,

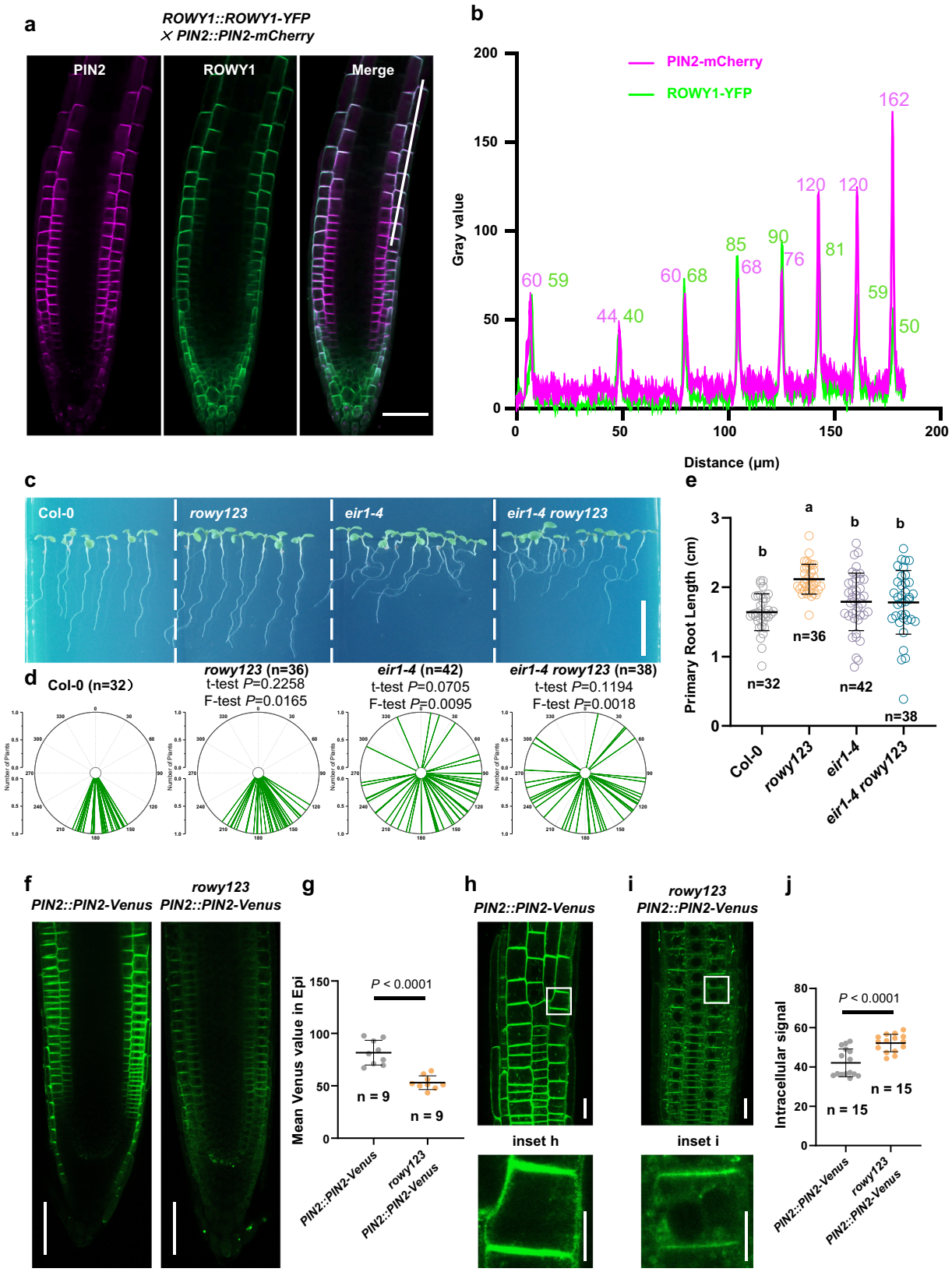

there was a greater intracellular distribution of PIN2. Thus, we hypothesize that ROWYs are positive regulators of PIN2 polar PM targeting. However, the roots of *rowy123* bent faster than did those of the WT, suggesting a potential regulatory mechanism for PIN2 protein homeostasis at the PM to avoid overbending. Notably, there was a decrease in DR5 redistribution in *rowy123* during the root gravitropic response, suggesting the presence of additional regulatory layers for the maintenance of maximal auxin in the root tips. In addition, PIN3 expression decreased in the root stele, and the decreased DR5 signal could be a combination of both basipetal shootward auxin transport and rootward auxin transport in the

Fig. 4 | ROWY1 colocalized with PIN2 and regulated its subcellular distribution. **a**, **b** ROWY1 and PIN2 colocalized in root epidermal cells. **a** Coexpression of PIN2-mCherry (left) and ROWY1-YFP (middle) in the primary root. Merged image of PIN2-mCherry and ROWY1-YFP (right). Track 1: laser wavelength, 594 nm, 40.00%; 0.0% offset; detector gain, 650 V. Track 2: laser wavelength, 488 nm, 20.00%; 0.0% offset; detector gain, 650 V. The white line indicates the plot area. Scale bar, 50 μm. **b** The gray value was measured to indicate the fluorescence intensity. Fluorescence plots and measurements were performed via ImageJ. **c**–**e** PIN2 and ROWYs play a role in the same signaling pathway. **c** Representative images showing comparisons of 7-day-old Col-0, *rowy123*, *eir1-4*, and *eir1-4 rowy123* seedlings. Scale bar, 1 cm. **d** The angles of the primary root tips of 7-day-old seedlings were measured and are shown as a polar histogram. *n* values are indicated. **e** The primary root length of 7-day-old seedlings was measured. The data are presented as the means ± SDs; *n* values are indicated. The experiments were repeated three times independently, with similar results obtained. **f**–**j** Loss of function of *ROWYs* impaired the subcellular distribution of PIN2. **f** Representative images showing *PIN2::PIN2-Venus* expression in the epidermal cells of Col-0 and *rowy1-1 rowy2-2 rowy3-2*. Four-day-old seedlings were grown constantly on MS media; laser wavelength, 488 nm, 10.00%; 0.0% offset; detector gain, 650 V; scale bar, 50 μm. **g** The mean value was measured to indicate the expression of PIN2 in epidermal cells; *n* values are indicated. *P* values were calculated with a two-tailed *t* test. **h** Representative images showing the epidermal cells of *PIN2::PIN2-Venus*. **i** Representative images showing the epidermal cells of *PIN2::PIN2-Venus;rowy123*. Insets represent enlargements of the boxed regions from the corresponding images. Laser wavelength, 488 nm, 10.00%; 0.0% offset; detector gain, 650 V. Scale bar, 20 μm. **j** The mean value was measured to indicate the intracellular signal; *n* values are indicated. *P* values were calculated with a two-tailed *t* test. The experiments were repeated four times independently, with similar results obtained.

root tips, suggesting the potential involvement of additional PIN auxin transporters.

ROWY1 is polarly distributed at the apical side of the PM in the root epidermis, where PIN2 also resides. The PM targeting of ROWY1 relies on its S-acylation at the C3 residue. However, disruption of S-acylation by amino acid substitution or chemical inhibition does not seem to be required for the biological function of ROWY1 in root growth. Together with the previous finding that ROWY1 might function as a negative regulator of the ESCRT complex at MVB/LE/PVC[52], we speculate that PM recycling from MVB/LE/PVC might function as a negative regulatory mechanism for ROWY1. Whether this type of posttranslational modification is responsive to external or internal cues might be an interesting open question awaiting further investigation.

Iron is an important nutrient for plant growth and development[56]. Here, we revealed that Fe^{2+} availability is a key regulator of wavy root growth. Notably, multiple related genes were upregulated in the *rowy123* triple mutant, and Fe^{2+} availability strikingly shaped the root system architecture, resembling *rowy123*. Notably, Fe^{2+} availability also modulates PIN2 subcellular distribution and related auxin distribution. Therefore, we propose that ROWY proteins are regulators of the Fe^{2+} homeostasis pathway. These data identify ROWYs as molecular hubs linking Fe nutrients to root growth, but the detailed molecular mechanisms involved require further research. A recent study revealed that *ROWY3* (*AtBro1*) might be involved in ABA signaling and the abiotic stress response[53]. Interestingly, all three *ROWY* genes are predicted to have multiple splice variants, and whether alternative splicing plays a role in regulating *ROWY3* function awaits further investigation.

Methods

Plant materials and growth conditions

Chlorine-sterilized *Arabidopsis* seeds were subsequently grown on ½ MS media supplemented with 1% (w/v) sucrose and 0.8% plant agar (pH 5.8). After 2 days of cold treatment (4 °C), the seeds were moved to a growth chamber at 22 °C under a 16-h light/8-h dark photoperiod. After 7 days of growth on MS media, the seedlings were transferred to soil and allowed to grow under the same conditions for 2–3 months until the plants matured.

Single mutants *rowy1-1* (WiscDsLox412H04), *rowy1-2* (GABI_041F11), *rowy2-1* (SALK_035256), *rowy2-2* (SALK_038492), *rowy3-1* (SALK_204462C), and *rowy3-2* (SALK_063092) were obtained from the Nottingham Arabidopsis Stock Centre (NASC). The transfer DNA (T-DNA) insertion sites were verified via PCR. The fluorescent reporter lines *pPIN1::PIN1-GFP*[57], *pPIN2::PIN2-GFP*[58], *pPIN2::PIN2-Venus*[37], *pPIN2::PIN2-mCherry*[59], *pBRAF1::BRAF1-YFP*[52], *pPIN3::PIN3-GFP*[60], *pPIN7::PIN7-GFP*[60], and *DR5rev::GFP*[61] were reported previously. These reporters were introduced into the *rowy123* triple mutant background by crossing. The floral dip method was used for *Arabidopsis* transformation with *Agrobacterium tumefaciens strain* GV3101. The fluorescent reporter lines and Promoter::GUS transgenic lines for *ROWYs* were generated via transformation. The mutants and transgenic lines used in this study are listed in Supplementary Table 1. All compounds are listed in Supplementary Table 2. The primers used for identifying T-DNA insertion sites and genotyping cross lines are listed in Supplementary Table 3.

Molecular cloning

Restriction enzyme digestion or Gateway cloning was used to make constructs for transgenic plant generation. For restriction enzyme digestion, the restriction enzyme sites were added to DNA fragments via PCR and then cloned and inserted into the corresponding plasmids. For Gateway cloning, DNA fragments were first cloned and inserted into entry vectors via the BP reaction and then cloned and inserted into destination vectors via the LR reaction. Point mutagenesis was performed with a QuikChange II Site-Directed Mutagenesis Kit (200524, Agilent Technologies). All reagents, including restriction enzymes and Gateway clonases, are listed in Supplementary Table 2. The primers used for molecular cloning are listed in Supplementary Table 3. The resulting plasmids from this study are listed in Supplementary Table 4.

Quantitative RT–PCR (RT–qPCR) analysis

RT-qPCR was used to examine the transcripts of *ROWY1* ~ *ROWY3* in *rowy* mutants, with *ACTIN7* (*AT5G09810*) as an internal reference. In detail, total RNA was extracted from the indicated tissues via TRIzol (Invitrogen), and DNase was added to digest the genomic DNA. For RT-PCR, first-strand cDNA was generated via a HiScript III 1st Strand cDNA Synthesis Kit (Vazyme). PCR was performed to amplify the full-length CDSs of *ROWY1, ROWY2* and *ROWY3*. For RT-qPCR, 1 μg of each RNA sample was reverse transcribed (Takara). The resulting cDNA of the corresponding genes and *ACTIN7* was analyzed via SYBR Premix Ex Taq (Takara) with a Bio-Rad CFX Connect Real-Time System. The relative transcript levels of the examined genes were normalized to those of *ACTIN7*, calculated by setting the wild-type or a certain tissue as "1", and finally presented as the average ± standard deviation (s.d.) from three biological replicates. The primers used are listed in Supplementary Table 3.

Promoter::β-glucuronidase (GUS) histochemical staining

For the promoter–GUS fusion studies, 1.5-kilobase (kb) genomic DNA fragments containing the promoter regions of the *ROWY1, ROWY2*, and *ROWY3* genes were amplified via PCR and subcloned and inserted into a modified pCambia1300 binary vector[62] (the primers used for molecular cloning are listed in Supplementary Table 3). Positive transgenic lines were used for staining.

The plant materials (seedlings, rosette leaves, inflorescences, fruits, etc.) were incubated in freshly prepared staining solution (100 mM Na-phosphate buffer, 0.1% (v/v) Triton X-100, 0.5 mM potassium ferrocyanide, 0.5 mM potassium ferricyanide, 10 mM EDTA, pH 7.0) supplemented with 0.5 mg/ml X-Gluc at 37 °C for 2–3 h. Then, the stained materials were decolorized with 90% and 70% ethanol at room temperature until the chlorophyll was completely removed. Specifically, for the imaging of roots, the decolorized materials were mounted with a transparent liquid (chloral hydrate:H_2O:glycerol = 8:3:1).

Immunostaining

Four-day-old roots were immunostained as previously described[48]. Seedlings were fixed with PBS supplemented with 4% paraformaldehyde (PFA) for 1 h under vacuum. The seedlings were washed three times with PBS containing 0.1% Triton for 10 minutes, followed by washing three times with water containing 0.1% Triton for 10 min. After incubation with 2%

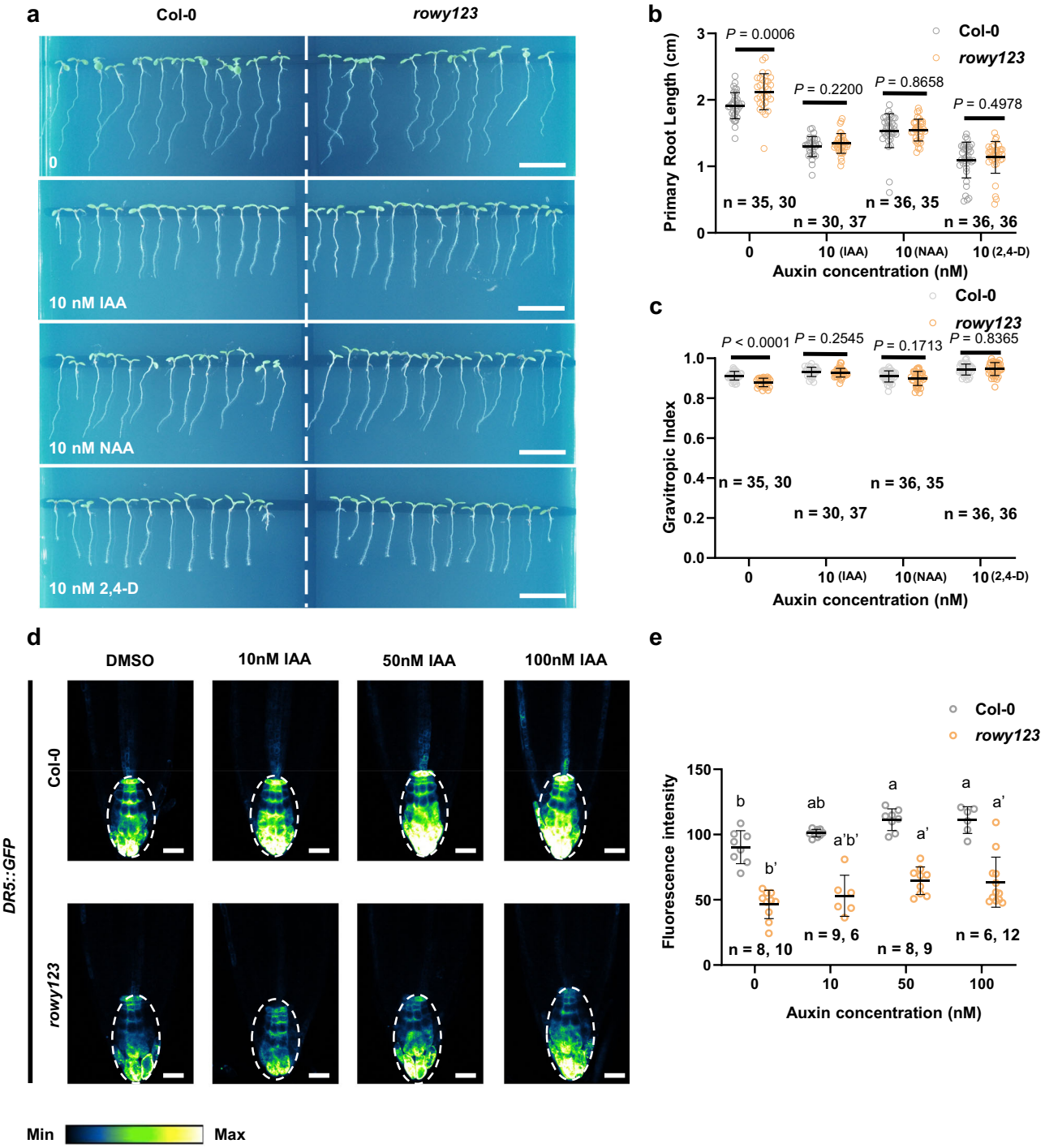

Fig. 5 | Exogenous auxin treatment rescued the wavy root phenotype of the *rowy123* mutant. a Representative images showing the morphological changes in 7-day-old Col-0 and *rowy123* seedlings grown on MS media supplemented with IAA, NAA, and 2,4-D at the indicated concentrations. DMSO was used as the solvent control. Scale bars, 1 cm. The experiments were repeated three times independently, with similar results obtained. **b** Exogenous auxin treatment rescued the primary root length of *rowy123* to a level similar to that of Col-0. **c** Exogenous auxin treatment reversed the wavy root phenotype of *rowy123*. Seven-day-old seedlings. The data are presented as the means ± SDs; *n* values are indicated. *P* values were calculated via a two-tailed t test for the indicated pairs of Col-0 and *rowy123* at the given concentrations. **d**, **e** The regular auxin-responsive pattern of *DR5rev::GFP* was reversed by IAA in *rowy123*. Four-day-old *DR5rev::GFP* seedlings grown on plates containing IAA at the indicated concentrations were imaged with CLSM. The dotted line circles indicate the regions used for quantification. The experiments were repeated three times independently, with similar results obtained. **d** Representative images of *DR5rev::GFP*. The fluorescence intensity is shown in dark blue, green, yellow, and white, with the fluorescence intensity increasing in turn. Laser wavelength, 488 nm, 14.00%; 0.0% offset; detector gain, 650 V. Scale bars, 20 μm. **e** Fluorescence intensity was measured to indicate reporter gene expression. The data are presented as the means ± SDs; *n* values are indicated. Different letters represent significant differences; $P < 0.05$; one-way ANOVA with multiple comparisons. The experiments were repeated three times independently, with similar results obtained.

driselase in PBS at 37 °C for 1 h, the seedlings were washed three times with PBS containing 0.1% Triton and then incubated with PBS supplemented with 10% DMSO and 3% NP40 at room temperature for 1 h. Seedlings were washed three times with PBS supplemented with 0.1% Triton for 10 min, followed by blocking with 2% bovine serum albumin (BSA) in PBS at room temperature for 1 h. Subsequently, the seedlings were incubated with a-GFP antibody (Sigma, 1:1000) in blocking solution at 37 °C for 4 h, followed by washing five times with PBS supplemented with 0.1% Triton for 10 min and incubation with Cy5-a-mouse antibody (1:600) in blocking solution at 37 °C for 4 h. The seedlings were washed three times with PBS containing 0.1% Triton for 10 min, followed by washing three times with water containing 0.1% Triton for 10 minutes. The samples were mounted in nonhardening mounting medium and imaged with an LSM 800 inverted confocal laser scanning microscope (Zeiss).

Fig. 6 | RNA-seq analysis revealed that *ROWYs* are related to the iron pathway. **a** Statistics of the results of the GO enrichment analysis of genes differentially expressed between Col-0 and *rowy123* plants. **b** Heatmap showing genes differentially expressed between Col-0 and *rowy123*, with upregulated genes in red and downregulated genes in blue. **c**–**e** Iron deficiency led to longer and wavy primary roots in *Arabidopsis* seedlings. **c** Representative images showing the morphological changes in 7-day-old Col-0 and *rowy123* seedlings grown on iron-deficient MS media. MS medium was used as the control. Scale bars, 1 cm. **d** The primary root length was measured. **e** The gravitropic index was measured to indicate the degree of bending. Seven-day-old seedlings. *n* values are indicated. Different letters represent significant differences; $P < 0.05$; one-way ANOVA with multiple comparisons. The experiments were repeated three times independently, with similar results obtained. **f**, **g** Iron deficiency disrupted the expression of PIN2. **f** Representative images showing *PIN2::PIN2-Venus* expression in epidermal cells of seedlings grown on iron-deficient MS media. Normal MS medium was used as the control. Laser wavelength, 488 nm, 5.00%; 0.0% offset; detector gain, 650 V. Scale bars, 50 μm. **g** The mean Venus value was measured to indicate the expression of PIN2 in epidermal cells. The data are presented as the means ± SDs; *n* values are indicated. *P* values were calculated with a two-tailed *t* test. The experiments were repeated four times independently, with similar results obtained.

Microscopy and image acquisition

For confocal laser-scanning microscopy (CLSM), a Zeiss LSM980 instrument equipped with a GaAsP detector (Zeiss) was used. Various confocal settings were set to record the emission of different fluorophores: EGFP (excitation, 488 nm; emission, 507 nm), YFP (excitation, 488 nm; emission, 527 nm), Venus (excitation, 488 nm; emission, 529 nm), mCherry (excitation, 543 nm; emission, 610 nm), mRFP (excitation, 543 nm; emission, 607 nm), and PI (excitation, 495 nm; emission, 635 nm). All of the images were obtained at an 8-bit depth with 2× line averaging.

The GUS-stained samples were imaged via a DIC microscope (Olympus BX53).

Phenotypic analysis

Col-0, *rowy1-1*, *rowy1-2*, *rowy2-1*, *rowy2-2* single mutants, *rowy1 rowy2*, *rowy2 rowy3*, *rowy1 rowy3* double mutants and *rowy1 rowy2 rowy3* triple mutants were uniformly seeded on 1/2 MS media. After 2 days of cold treatment (4 °C), the seeds were moved to the growth chamber, and the other conditions were completely consistent. After a certain number (as indicated in the figure legends) of days, MS plates were imaged with a Sony A6000 camera with a macro lens, and then the primary root length, growth distance, or root tip angles were analyzed with ImageJ software.

Pharmacological treatments and experimental conditions

For exogenous auxin treatments, *Arabidopsis* seeds were sown on MS plates supplemented with the indicated exogenous auxin, including IAA (Sigma), NPA (Sigma), and 2,4-D (Sigma). After stratification for 2 d at 4 °C, the plates were transferred to the growth chamber under the conditions described in the "Plant materials and growth conditions" section for 6 d according to different assays. The phenotype was then analyzed via ImageJ.

For short-term treatment to study the subcellular localization of PIN2::PIN2-Venus and PIN2::PIN2-Venus in *rowy123*, 4-day-old seedlings grown on normal MS plates were transferred to 100 μM BFA or 33 μM Wm liquid MS for 1 h. Afterwards, the samples were imaged via CLSM.

Accession numbers

The sequence data from this study can be found in the *Arabidopsis* Genome Initiative or enBank/EMBL databases. The accession numbers are as follows: *ROWY1* (*AT5G14020*), *ROWY2* (*AT1G17940*), *ROWY3* (*AT1G73390*), *PIN1* (*AT1G73590*), *PIN2* (*AT5G57090*), *PIN3* (*AT1G70940*), and *PIN7* (*AT1G23080*).

RNA-seq analysis

For RNA-seq analysis, the roots were cut from 7-day-old Col-0 and *rowy123* seedlings. Four independent RNA samples (100 mg) were used for the following analyses. RNA extraction and RNA-seq were performed by BGI via the BGISEQ platform. The reads of each sample were aligned to the publicly available reference genome of Arabidopsis (TAIR10, https://support.illumina.com/sequencing/sequencing_software/igenome.html) via HISAT2 version 2.0.4 with default parameters. Data analyses were performed with the Dr. Tom platform of BGI. The differentially expressed genes of Col-0 and *rowy123* with $\log2 > 0$ are listed in Supplementary Data 1. GO enrichment analysis was based on the classification of the GO_P term description as $\log2 > 0$. *P* values were calculated via the phyper function, and Q values were obtained via FDR correction of *P* values. Functions with a Q value $<= 0.05$ are considered significantly enriched. Heatmap analysis was performed via OECloud tools (https://cloud.oebiotech.com) as $\log2 >= 0.58$.

Statistics and reproducibility

Most experiments were repeated at least three times independently, with similar results obtained. The results are reported as the means ± SD. To measure primary root length, growth distance, and root-tip angles, photographs were analyzed via ImageJ (https://imagej.nih.gov/ij/download.html). The fluorescence intensity of the CLSM images was quantified via Fiji (https://fiji.sc/). Data visualization and statistical analysis were mostly performed with GraphPad Prism 8. For the bending curvatures of the roots, polar bar graphs were generated via Origin 2021. The *n* value represents the number of seedlings or independent experiments. *P* values were calculated with a two-tailed *t* test for quantitative variables between two independent groups or one-way ANOVA for quantitative variables among three or more independent groups. The results were considered statistically significant when the *p* value was less than 0.05.

Reporting summary

Further information on research design is available in the Nature Portfolio Reporting Summary linked to this article.

Data availability

The RNA-seq data for this study are available online at the NCBI Sequence Read Archive (accession number: PRJNA1116831). Uncropped images of the DNA gels are provided in the Supplementary Figs. 21 to 22. The source data used to generate the plots are provided in the Supplementary Data 2.

Received: 19 October 2023; Accepted: 18 August 2024;
Published online: 04 September 2024

References

1. Friml, J. Fourteen stations of auxin. *Cold Spring Harb. Perspect. Biol.* **14**, a039859 (2022).
2. Zhao, Y. Essential roles of local auxin biosynthesis in plant development and in adaptation to environmental changes. *Annu. Rev. Plant Biol.* **69**, 417–435 (2018).
3. Brumos, J. et al. Local auxin biosynthesis is a key regulator of plant development. *Dev. Cell* **47**, 306–318 (2018).
4. Robert, H. S. et al. Local auxin sources orient the apical-basal axis in *Arabidopsis* embryos. *Curr. Biol.* **23**, 2506–2512 (2013).
5. Adamowski, M. & Friml, J. PIN-dependent auxin transport: action, regulation, and evolution. *Plant Cell* **27**, 20–32 (2015).
6. Tan, S., Luschnig, C. & Friml, J. Pho-view of auxin: reversible protein phosphorylation in auxin biosynthesis, transport and signalling. *Mol. Plant* **14**, 151–165 (2021).
7. Lavy, M. & Estelle, M. Mechanisms of auxin signaling. *Development* **143**, 3226–3229 (2016).
8. Gallei, M., Luschnig, C. & Friml, J. Auxin signalling in growth: Schrödinger's cat out of the bag. *Curr. Opin. Plant Biol.* **53**, 43–49 (2020).

9. Stepanova, A. N. et al. TAA1-mediated auxin biosynthesis is essential for hormone crosstalk and plant development. *Cell* **133**, 177–191 (2008).
10. Tao, Y. et al. Rapid synthesis of auxin via a new tryptophan-dependent pathway is required for shade avoidance in plants. *Cell* **133**, 164–176 (2008).
11. He, W. et al. A small-molecule screen identifies l-kynurenine as a competitive inhibitor of TAA1/TAR activity in ethylene-directed auxin biosynthesis and root growth in *Arabidopsis*. *Plant Cell* **23**, 3944–3960 (2011).
12. Salehin, M., Bagchi, R. & Estelle, M. SCF TIR1/AFB-based auxin perception: mechanism and role in plant growth and development. *Plant Cell* **27**, 9–19 (2015).
13. Li, L., Gallei, M. & Friml, J. Bending to auxin: fast acid growth for tropisms. *Trends Plant Sci.* **27**, 440–449 (2022).
14. Qi, L. et al. Adenylate cyclase activity of TIR1/AFB auxin receptors in plants. *Nature* **611**, 133–138 (2022).
15. Lin, W., Tang, W., Takahashi, K., Ren, H. & Pan, S. TMK-based cell surface auxin signaling activates cell wall acidification in Arabidopsis. *Nature* **599**, 278–282 (2021).
16. Friml, J. et al. ABP1-TMK auxin perception mediates ultrafast global phosphorylation and auxin canalization. *Nature* **609**, 575–581 (2022).
17. Petrášek, J. et al. PIN proteins perform a rate-limiting function in cellular auxin efflux. *Science* **312**, 914–918 (2006).
18. Yang, Z. et al. Structural insights into auxin recognition and efflux by Arabidopsis PIN1. *Nature* **609**, 611–615 (2022).
19. Lam Ung, K. et al. Structures and mechanism of the plant PIN-FORMED auxin transporter. *Nature* **609**, 605–610 (2022).
20. Su, N. et al. Structures and mechanisms of the Arabidopsis auxin transporter PIN3. *Nature* **609**, 616–621 (2022).
21. Xia, J. et al. Chemical inhibition of Arabidopsis PIN-FORMED auxin transporters by the anti-inflammatory drug naproxen. *Plant Commun.* **6**, 100632 (2023).
22. Konstantinova, N. et al. WAVY GROWTH Arabidopsis E3 ubiquitin ligases affect apical PIN sorting decisions. *Nat. Commun.* **13**, 5147 (2022).
23. Hao, P. et al. Auxin-transporting ABC transporters are defined by a conserved D/E-P motif regulated by a prolylisomerase. *J. Biol. Chem.* **295**, 13094–13105 (2020).
24. Serrano, M. et al. Export of salicylic acid from the chloroplast requires the multidrug and toxin extrusion-like transporter EDS5. *Plant Physiol.* **162**, 1815–1821 (2013).
25. Ying, W. et al. Structure and function of the Arabidopsis ABC transporter ABCB19 in brassinosteroid export. *Science* **383**, eadj4591 (2024).
26. Marchant, A. et al. AUX1 regulates root gravitropism in Arabidopsis by facilitating auxin uptake within root apical tissues. *EMBO J.* **18**, 2066–2073 (1999).
27. Ung, K. L., Schulz, L., Pedersen, B. P., Stokes, D. L. & Hammes, U. Z. Substrate recognition and transport mechanism of the PIN-FORMED auxin exporters. *Trends Biochem. Sci.* **48**, 937–948 (2023).
28. Luschnig, C., Gaxiola, R. A., Grisafi, P. & Fink, G. R. EIR1, a root specific protein involved in auxin transport, is required for gravitropism in *Arabidopsis thaliana*. *Genes Dev.* **12**, 2175–2187 (1998).
29. Cheng, Y., Qin, G., Dai, X. & Zhao, Y. NPY genes and AGC kinases define two key steps in auxin-mediated organogenesis in *Arabidopsis*. *Proc. Natl Acad. Sci. USA* **105**, 21017–21022 (2008).
30. Dhonukshe, P. et al. Plasma membrane-bound AGC3 kinases phosphorylate PIN auxin carriers at TPRXS(N/S) motifs to direct apical PIN recycling. *Development* **137**, 3245–3255 (2010).
31. Glanc, M. et al. AGC kinases and MAB4/MEL proteins maintain PIN polarity by limiting lateral diffusion in plant cells. *Curr. Biol.* **31**, 1918–1930.e5 (2021).
32. Glanc, M., Fendrych, M. & Friml, J. Mechanistic framework for cell-intrinsic re-establishment of PIN2 polarity after cell division. *Nat. Plants* **4**, 1082–1088 (2018).
33. Sakai, T. et al. The WAVY GROWTH 3 E3 ligase family controls the gravitropic response in *Arabidopsis* roots. *Plant J.* **70**, 303–314 (2012).
34. Semeradova, H., Montesinos, J. C. & Benkova, E. All roads lead to auxin: post-translational regulation of auxin transport by multiple hormonal pathways. *Plant Commun.* **1**, 100048 (2020).
35. Marhavý, P. et al. Cytokinin controls polarity of PIN1-dependent Auxin transport during lateral root organogenesis. *Curr. Biol.* **24**, 1031–1037 (2014).
36. Li, L., Xu, J., Xu, Z. H. & Xue, H. W. Brassinosteroids stimulate plant tropisms through modulation of polar auxin transport in *Brassica* and *Arabidopsis*. *Plant Cell* **17**, 2738–2753 (2005).
37. Retzer, K. et al. Brassinosteroid signaling delimits root gravitropism via sorting of the *Arabidopsis* PIN2 auxin transporter. *Nat. Commun.* **10**, 5516 (2019).
38. Du, Y. et al. Salicylic acid interferes with clathrin-mediated endocytic protein trafficking. *Proc. Natl Acad. Sci. USA* **110**, 7946–7951 (2013).
39. Huang, D. et al. Salicylic acid-mediated plasmodesmal closure via Remorin-dependent lipid organization. *Proc. Natl Acad. Sci. USA* **116**, 21274–21284 (2019).
40. Ke, M. et al. Salicylic acid regulates PIN2 auxin transporter hyperclustering and root gravitropic growth via Remorin-dependent lipid nanodomain organisation in *Arabidopsis thaliana*. *N. Phytol.* **229**, 963–978 (2021).
41. Tan, S. et al. Salicylic Acid targets Protein Phosphatase 2A to attenuate growth in plants. *Curr. Biol.* **30**, 381–395.e8 (2020).
42. Pasternak, T. et al. Salicylic acid affects root meristem patterning via auxin distribution in a concentration-dependent manner. *Plant Physiol.* **180**, 1725–1739 (2019).
43. Li, Y. et al. Root growth adaptation is mediated by PYLs ABA receptor-PP2A protein phosphatase complex. *Adv. Sci.* **7**, 1901455 (2020).
44. Zhang, J. et al. The ABI3-ERF1 module mediates ABA-auxin crosstalk to regulate lateral root emergence. *Cell Rep.* **42**, 112809 (2023).
45. Sun, J. et al. Jasmonate modulates endocytosis and plasma membrane accumulation of the *Arabidopsis* PIN2 protein. *N. Phytol.* **191**, 360–375 (2011).
46. Zhang, J. et al. Strigolactones inhibit auxin feedback on PIN-dependent auxin transport canalization. *Nat. Commun.* **11**, 3508 (2020).
47. Ötvös, K. et al. Modulation of root growth by nutrient-defined fine-tuning of polar auxin transport. *EMBO J.* **40**, e106862 (2021).
48. Baster, P. et al. SCFTIR1/AFB-auxin signalling regulates PIN vacuolar trafficking and auxin fluxes during root gravitropism. *EMBO J.* **32**, 260–274 (2013).
49. Platre, M. P. et al. Developmental control of plant Rho GTPase nano-organization by the lipid phosphatidylserine. *Science* **364**, 57–62 (2019).
50. Leitner, J. et al. Lysine63-linked ubiquitylation of PIN2 auxin carrier protein governs hormonally controlled adaptation of *Arabidopsis* root growth. *Proc. Natl Acad. Sci. USA* **109**, 8322–8327 (2012).
51. Shih, H. W., Depew, C. L., Miller, N. D. & Monshausen, G. B. The cyclic nucleotide-gated channel CNGC14 regulates root gravitropism in *Arabidopsis thaliana*. *Curr. Biol.* **25**, 3119–3125 (2015).
52. Shen, J. et al. A plant Bro1 domain protein BRAF regulates multivesicular body biogenesis and membrane protein homeostasis. *Nat. Commun.* **9**, 3784 (2018).
53. Mehdi, S. M. M., Szczesniak, M. W. & Ludwików, A. The Bro1-like domain-containing protein, AtBro1, modulates growth and abiotic stress responses in Arabidopsis. *Front. Plant Sci.* **14**, 1157435 (2023).
54. Gollhofer, J., Timofeev, R., Lan, P., Schmidt, W. & Buckhout, T. J. Vacuolar-Iron-Transporter1-like proteins mediate iron homeostasis in Arabidopsis. *PLoS ONE* **9**, e110468 (2014).

55. Zhao, X. et al. NITRIC OXIDE-ASSOCIATED PROTEIN1 (AtNOA1) is essential for salicylic acid-induced root waving in *Arabidopsis thaliana*. *N. Phytol.* **207**, 211–224 (2015).
56. Chen, C. C., Chien, W. F., Lin, N. C. & Yeh, K. C. Alternative functions of Arabidopsis YELLOW STRIPELIKE3: from metal translocation to pathogen defense. *PLoS ONE* **9**, e98008 (2014).
57. Benková, E. et al. Local, efflux-dependent auxin gradients as a common module for plant organ formation. *Cell* **115**, 591–602 (2003).
58. Xu, J. & Scheres, B. Dissection of *Arabidopsis* ADP-RIBOSYLATION FACTOR 1 function in epidermal cell polarity. *Plant Cell* **17**, 525–536 (2005).
59. Salanenka, Y. et al. Gibberellin DELLA signaling targets the retromer complex to redirect protein trafficking to the plasma membrane. *Proc. Natl Acad. Sci. USA* **115**, 3716–3721 (2018).
60. Zadnikova, P. et al. Role of PIN-mediated auxin efflux in apical hook development of *Arabidopsis thaliana*. *Development* **137**, 607–617 (2010).
61. Friml, J. et al. Efflux-dependent auxin gradients establish the apical-basal axis of Arabidopsis. *Nature* **426**, 147–153 (2003).
62. Liu, W., Xu, Z. H., Luo, D. & Xue, H. W. Roles of OsCKI1, a rice casein kinase I, in root development and plant hormone sensitivity. *Plant J.* **36**, 189–202 (2003).

Acknowledgements

We thank Drs. Erika Isono (University of Constance), Grégory Vert (University of Toulouse), and Liwen Jiang (The Chinese University of Hong Kong) for kindly sharing published *Arabidopsis* lines; Dr. Yuzhou Zhang (ISTA) for help with molecular cloning, and Drs. Melinda Abas (BOKU), Eugenia Russinova (Ghent University), and Zhaojun Ding (Shandong University) for valuable discussions. This work was supported by grants to S.T. from the National Natural Science Foundation of China (32321001), the USTC Research Funds of the Double First-Class Initiative (YD9100002016), the Research Funds from the Center for Advanced Interdisciplinary Science and Biomedicine of IHM, the Division of Life Sciences and Medicine, the University of Science and Technology of China (QYPY20220012), the Fundamental Research Funds for the Central Universities (WK9100000021), and start-up funding from the University of Science and Technology of China and the Chinese Academy of Sciences (GG9100007007, KY9100000026, KY9100000051, and KJ2070000079). J.S. was supported by the National Natural Science Foundation of China (31970181 and 32170342). J.F. was supported by Austrian Science Fund (FWF; projects I6123 and P37051-B).

Author contributions

S.T. conceived the project and designed the experiments. The project was initiated by S.T. in the J.F. lab. Y.P., K.J., Y.M., and Y.W. performed the physiological and cellular experiments under supervision of S.T., J.F., and E.B. All the authors contributed to the data analysis. B.K., C.L., and J.S. contributed reporter lines and provided critical suggestions. Y.P., J.F., and S.T. wrote the manuscript with input from other coauthors, and all authors revised and approved the submitted version.

Competing interests

The authors declare no competing interests.

Additional information

Supplementary information The online version contains supplementary material available at https://doi.org/10.1038/s42003-024-06747-9.

Correspondence and requests for materials should be addressed to Shutang Tan.

Peer review information *Communications Biology* thanks Ranjan Swarup and the other, anonymous, reviewer(s) for their contribution to the peer review of this work. Primary Handling Editor: David Favero. A peer review file is available.